Cellular Physiology and Biochemistry

Cell Physiol Biochem 2018;45:332-342
DOI: 10.1159/000486814
Published online: January 24, 2018
Accepted: December 09, 2017







**Original Paper**

# NF-κB-Induced MicroRNA-211 Inhibits Interleukin-10 in Macrophages of Rats with Lipopolysaccharide-Induced Acute Respiratory Distress Syndrome

Shengyun Wang[a] Zhenjie Li[b] Qitong Chen[a] Lv Wang[a] Jinhao Zheng[a] Zhaofen Lin[a] Wenfang Li[a]

[a]Department of Emergency and Critical Care Medicine, Changzheng Hospital, Second Military Medical University, Shanghai, [b]Department of Anesthesiology, Changzheng Hospital, Second Military Medical University, Shanghai, China

**Key Words**
Ards • MiR-211 • IL-10 • NF-κB • Macrophage

**Abstract**
***Background/Aims:*** The present study addressed the potential involvement of microRNAs in acute respiratory distress syndrome (ARDS)-related inflammation and elucidates the underlying molecular mechanism. ***Methods:*** ARDS rat model was established by lipopolysaccharide, with compromised gas exchange capacity and lung edema. The inflammatory cells from bronchoalveolar lavage fluid (BALF) were profiled with automatic blood cell analyzer. The relative fluorescence intensity of BALF-derived macrophages was analyzed by flow cytometry. The relative microRNA expression was determined using microarray and Taqman assay. The secretory interleukin (IL)-10 was measured by enzyme-linked immunosorbent assay. Luciferase reporter assay was performed to determine the regulatory effects of miR-211 and NF-κB on IL-10 and miR-211 expressions, respectively. Chromatin immunoprecipitation (ChIP) was conducted to detect the direct binding of NK-κB on miR-211 promoter. The protein level was determined by Western blot. ***Results:*** The provoked acute inflammation was characterized with increased total cells, macrophages, neutrophils and lymphocytes. The relative expression of miR-211 was aberrantly up-regulated in BALF-derived macrophages from ARDS rats, which was accompanied with reduction of secretory IL-10. We further demonstrated that miR-211 inhibited IL-10 expression by binding to its 3'-UTR. The expression of miR-211 was modulated by NF-κB. ***Conclusion:*** Here we elucidated a crucial role of NF-κB/miR-211/IL-10 signaling axis in ARDS-related inflammation.



S. Wang and Z. Li contributed equally to this work.

Wenfang Li
and Zhaofen Lin

Department of Emergency and Critical Care Medicine, Changzheng Hospital
Second Military Medical University, 415 Fengyang Road, Shanghai (China)
E-Mail chzhedlwf@smmu.edu.cn, linzhaofen@smmu.edu.cn

## Introduction

The acute respiratory distress syndrome (ARDS) refers to the critical medical condition characterized by serious inflammatory reaction in the lung, which may be caused by a range of diseases such as trauma, pneumonia and sepsis [1]. The clinical manifestations of ARDS include diffuse injury to the alveolar barrier cells, surfactant dysfunction, active innate immune response and unusual coagulation, which consequently and convergently result in the impairment of gas exchange function in the alveoli [2]. ARDS is associated with an extremely poor prognosis and a mortality of 20%~50% worldwide [3]. At the molecular level, inflammation reaction triggered by the acute lung injury and the chemical signals and inflammatory mediators subsequently secreted by the epithelial and endothelial cells are the hallmarks of ARDS [4]. Neutrophils and some of the lymphocytes recruited via chemotaxis further exacerbate this phenomenon [5]. Despite tremendous advance in our understanding of the ARDS pathology in the past decades, the detailed regulatory network underlying the inflammation response in this disease is still elusive. Here we set out to investigate the potential involvement of microRNAs in the pathogenesis of ARDS in lipopolysaccharide (LPS)-induced rat model and to further elucidate its associated molecular events.

MicroRNAs (miRNAs, miRs) are a class of small non-coding RNA molecules with an average length of 22 nucleotides and widely exist in plants, virus and animals [6]. The considerable range of critical physiological functions of miRNAs have been disclosed, most of which greatly rely on its fine-tuned gene regulation via either mRNA degradation or translation blockade [7]. Theoretically, a single miRNA simultaneously modulates expressions of hundreds of genes in a synergistic or antagonistic way with other miRNAs. All these modes of actions constitute a complicated, multi-node and multi-layer regulatory network. In addition to its normal functions, assembling evidences suggest that miRNA are also involved in various pathological conditions such as cardiomyopathies [8], atherosclerosis [9], obesity [10] and cancer [11]. Most importantly, emerging evidences suggest that miRNAs play crucial roles in inflammation responses [12], as well as in acute lung injury and ARDS [13].

In this study, we employed the well-acknowledged protocol to establish ARDS model via intratracheal instillation of cytotoxic LPS [14], which elicited acute inflammatory reaction in the lung tissues and well recapitulated the pathological progress of ARDS. LPS administration provoked severe respiratory distress indicated by the declined air exchange capacity and lung edema. The ARDS associated inflammatory reactions were extremely stimulated with overt shift in immune cell profiles. Noteworthily, we focused our mechanistic investigations on ARDS-derived macrophages, which are the key mediator in inflammatory environment. The miRNA microarray technology was employed in this study to identify candidate miRNAs involved in the pathological process of ARDS-associated inflammation, and subsequent customized miRNA assay for confirmation. Both the upstream and downstream molecular events were extendedly elucidated along the miR-211 axis. Therefore, we proposed a critical role of NF-κB/miR-211/interleukin (IL)-10 signaling pathway in ARDS-related inflammation, which provided further understanding of the molecular mechanism underlying the disease.

## Materials and Methods

*ARDS rat model LPS-induced ARDS model in rats*

5-week old male Wistar rats with body weight range of 200±15 g were obtained from the Shanghai Laboratory Animal Center (SLAC) and maintained in pathogen-free environment. The ARDS model was established following the well-established protocol [14]. Briefly, n=12 rats were included in each LPS treatment group and control group, in three independent repeats. The rats were anesthetized with 3% sodium pentobarbital and LPS (Escherichia coli O111:B4 dissolved in saline; Sigma, St. Louis, MO, USA) was administrated by intratracheal instillation at the dose of 2 mg/kg. The rats were positioned upright to ensure evenly distribution of LPS (LPS treatment group) or saline (control group) in bilateral lung tissues. The blood samples were collected from abdominal aorta at 2, 6 and 12 hours after administration. All animal

experiments were conducted in strict accordance with protocol approved by the Institutional Committee of Animal Care and Use of Changzheng Hospital, Second Military Medical University.

*Arterial blood gas analysis and lung wet-dry ratio*

The arterial blood samples were collected at the indicated time point and $PaO_2$, $PaCO_2$ were measured with the automatic blood gas Analyzer ABL800 flex (Radiometer). The alveolar-arterial oxygen tension difference [P(A-a) $O_2$] was calculated with the standard alveolar gas equation assuming respiratory quotient of 1.0. The oxygenation index was expressed as ratio between $PaO_2$ and $FiO_2$. The lung was excised and weighed immediately after the mice were sacrificed. The dry weight of lung was re-measured after 72 hours of dehydration in 60°C oven. The wet-dry ratio was calculated.

*Analysis of lung inflammatory cells*

The total and differential counts of leukocytes were measured with automatic blood cell analyzer (Sysmex). The results represented three independent repeats. The relative fluorescence intensity of macrophages was analyzed with flow cytometry. Totally, 10, 000 viable cells were scored for each measurement. All cell debris and dead cells were excluded by threshold gating. The fluorescence intensity (FI) and side scatter (SS) were recorded.

*Isolation of macrophages from BALF*

4 days after LPS treatment, BAL was performed using 2 ml of saline at ambient temperature. The saline was retrieved into a 4 ml polystyrene vacuum-bottle (Busse Hospital Disposable). The sample was immediately diluted with 3 volumes of phosphate-buffered saline (PBS) and transferred to 15 ml polypropylene tube. After brief chilling, the single-cell suspension was passed through a 110 μm cell strainer. The alveolar mononuclear leukocytes were then isolated with commercial kit (Genmed Scientifics)

*Macrophage culturing*

The freshly prepared BALF macrophage was washed with ice-cold PBS and resuspended in RPMI-1640 (Gibco, Grand Island, NY, USA) to final density of 1×106 cells/ml. The complete medium contained 10% normal rat serum and 1% PSG (penicillin-streptavidin-glutamine). Cells were maintained in 37°C humidified incubator supplied with 5 % $CO_2$.

*MiRNA microarray*

Total RNA was extracted from BALF macrophages using Trizol (Invitrogen, Carlsbad, CA, USA) and the quantity and quality was first determined by BioAnalyzer 2100 (Agilent, Santa Clara, CA). Reverse transcription was performed with the SuperScript II Reverse Transcriptase (ThermoFisher) and biotin labeling was performed with the BioArray High Yield RNA Transcript Labeling kit (Enzo). The hybridization steps were performed on the hybridization station (Tecan) followed by an indirect detection of streptavidin-Alexa647 conjugate (ThermoFisher Scientific, S21374, USA). The image was analyzed by GenePix pro (Molecular Devices, Sunnyvale, CA, USA). The U6 small RNA was employed as reference. Approximately 400 miRNAs were represented in the microarray. The expression of candidate miRs were further confirmed with customized mature miR microarray.

*MiRNA assays*

Expression of miR-211-5p was analyzed using Taqman Advanced miRNA assay kit (478507_mir) from ThermoFisher Scientific (Waltham, MA USA). The MISSION Lenti miR-211-5p mimic (HLMIR0374) from Sigma-Aldrich (St. Louis, MO, USA) was used for stable expression in cells following manufacturer's manuals.

*Enzyme-linked immunosorbent assay (ELISA)*

The secretory interleukin (IL)-10 in BALF macrophage culture medium was determined by ELISA (BMS629, ThermoFisher, USA) in accordance with the manufacturer's instruction.

*Luciferase assay*

The wild-type or putative target site mutated 3'UTR of IL-10 was cloned into the luciferase reporter plasmid. Both miR-211 mimic and luciferase reporter plasmid were co-transfected into BALF macrophage.

The relative luciferase activity was determined 24-hour post-transfection with the Dual Luciferase Assay System (Promega, Madison, WI, USA).

*Chromatin immunoprecipitation (ChIP)*

The exponential BALF macrophages were cross-linked with 4 % formaldehyde for one hour, followed by ultrasonication on ice. The DNA fragments immunoprecipitated with p65 antibody were recovered by denaturing. The primer sequences used for ChIP assay were available upon request. Binding efficiency (Bound/RPII%) was calculated as the amplification efficiency ratio between p65 and polymerase RNA II.

*Western blot*

Cell lysates were prepared in lysis buffer. Protein concentration was determined using bicinchoninic acid protein assay (ThermoFisher, USA). Equal amount of proteins was resolved by sodium dodecyl sulfate polyacrylamide gel electrophoresis and transferred onto polyvinylidene difluoride (PVDF) membrane in ice-bath. Blocking was performed with 5 % skim milk in Tris-buffered saline with0.05 % Tween-20 (TBST) for one hour at room temperature. The PVDF membrane was incubated with indicated primary antibodies (IκBα, CST #4814, 1:1, 000; Phospho-IκBα (Ser32), CST #5209, 1:1, 000; NF-κB p65 (D14E12), CST#8242, 1:1, 000; β-Actin (8H10D10), CST#3700, 1:1, 000) at 4□ overnight. After rigorous wash with TBST for 6×5 min, the membrane was subjected to secondary antibody (HRP-conjugated Anti-rabbit IgG, 1:3, 000; HRP-conjugated Anti-mouse IgG, 1:3, 000) hybridization. The unbound antibodies were completely washed off and protein bands were visualized by enhanced chemiluminescence method (Millipore, Billerica, MA, USA). β-actin was employed as loading control.

*Statistical analysis*

The statistical analysis in this study was performed using SPSS 23.0. All results were obtained from at least three independent repeats and presented as mean ± standard deviation (SD). T-test was employed for pairwise comparison and p value was calculated with $p < 0.05$ considered as statistically different.

## Results

*Establishment of the ARDS model by LPS induction*

We have established ARDS rat model by LPS induction in accordance with the well-established protocol [14]. To further evaluate the success of our system, here we first set out to examine the pulmonary functions by measuring [P(A-a) $O_2$] and $PaO_2/FiO_2$ ratio at 4 hour post-administration of LPS. Our results demonstrated a remarkable increase in [P(A-a) $O_2$] in the LPS group compared to the control group (Fig. 1A), and $PaO_2/FiO_2$ ratio was significantly decreased in response to LPS treatment (Fig. 1B). Moreover, the weight ratio between wet and dry lung excised from the same rat was notably higher in the LPS group (Fig. 1C), which

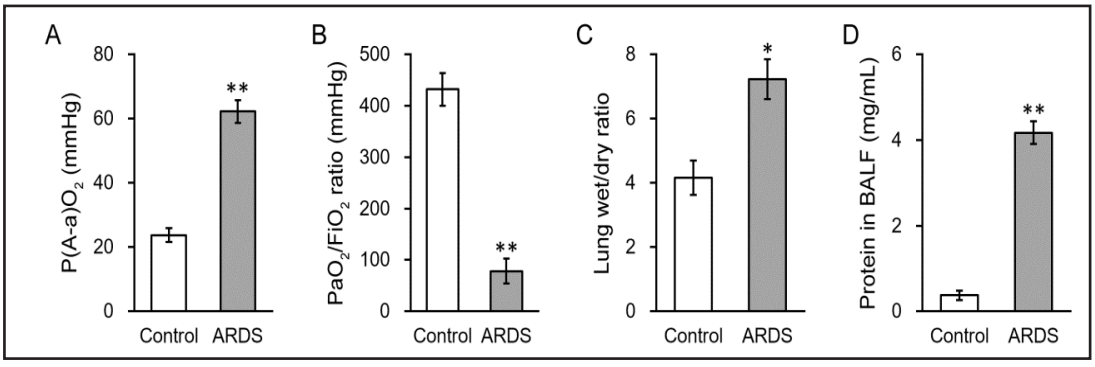


**Fig. 1.** Establishing the ARDS rat model. LPS-induced lung impairments in experimental rats, as characterized by P(A-a)$O_2$ (A), $PaO_2/FiO_2$ ratio (B), lung wet/dry ratio (C) and protein contents in BALF (D). Data were shown as mean±SD (n=12 each group). * $p<0.05$, ** $p<0.01$, compared to control.

indicated apparent pulmonary edema. This observation was further consolidated by the increase of protein concentration in BALF from the LPS-treated rats (Fig. 1D). Taken together, here we confirmed our success in recapitulating ARDS symptoms in the ARDS rat model.

*Inflammatory cell profiles in BALF of LPS-induced ARDS rats*

To further characterize the immune cell profile and inflammation response in LPS-induced ARDS, here we analyzed the total and indicated inflammatory cell levels 4 days after LPS treatment. Numbers of total cells (Fig. 2A), macrophages (Fig. 2B), neutrophils (Fig. 2C) and lymphocytes (Fig. 2D) were significantly enriched in BALF from LPS-induced ARDS rats. Notably, the influx of neutrophils was extremely higher in ARDS model in comparison with the control group. Our data suggested severe pulmonary inflammatory reaction in the established ARDS model.

*Flow cytometry profiles of monocytes and macrophages isolated from BALF of experimental rats*

Next, we focused on macrophages due to its well-acknowledged roles in acute inflammatory response [15]. As shown in Fig. 2B, the number of macrophages manifested approximate 5-fold increase in LPS-induced ARDS rats. Both monocytes and macrophages were isolated from BALF of either LPS or control rats. The fluorescence intensity and side scatter were quantitatively measured and compared between macrophages and monocytes. As illustrated in Fig. 2E, the spontaneous fluorescence signal was markedly higher in macrophages than monocytes. Similarly, macrophages displayed a higher level of side scatter, which indicated more complex composition of macrophages in this setting.

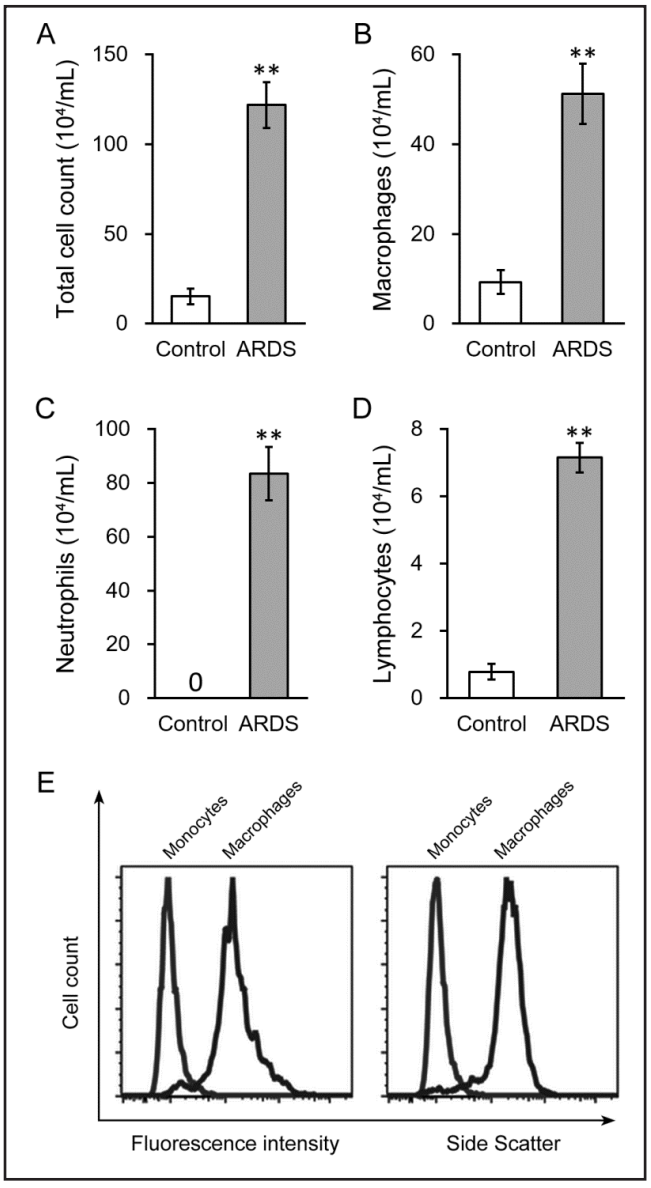


**Fig. 2.** Immune cell profiles in BALF of ARDS rats. BALF was collected 24 h post LPS treatment. Immune cell profiles were analyzed by the numbers of total cells (A), macrophages (B), neutrophils (C) and lymphocytes (D). Data were shown as mean±SD (n=12 each group). ** $p<0.01$, compared to control. (E) Flow cytometry profiles of monocytes and macrophages isolated from BALF of experimental rats, analyzed by flow cytometry based on differences in relative fluorescence intensity (log scale; left panel) and relative side scatter (log scale; right panel).

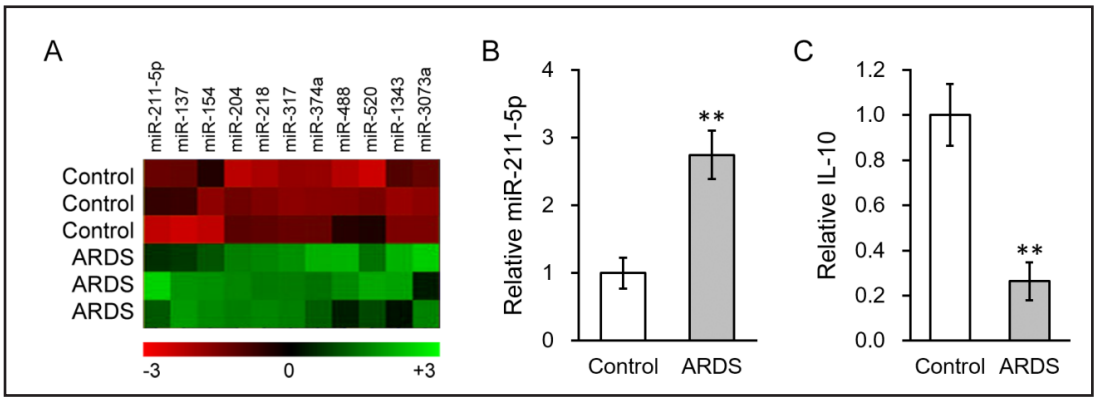


**Fig. 3.** MicroRNA expression profile in isolated BALF macrophages. (A) Macrophages isolated from BALF of control and ARDS rats, respectively, were subjected to miRNA microarray analysis, and miRNAs upregulated in ARDS compared to control were listed. (B) Expressions of miR-211-5p were analyzed by mature miRNA assay in macrophages isolated from BALF of control and ARDS rats, respectively. (A) IL-10 secretion from the macrophages isolated from BALF of control and ARDS rats, respectively, were analyzed by ELISA assay. Data were shown as mean±SD from at least three independent experiments. ** p<0.01, compared to control.

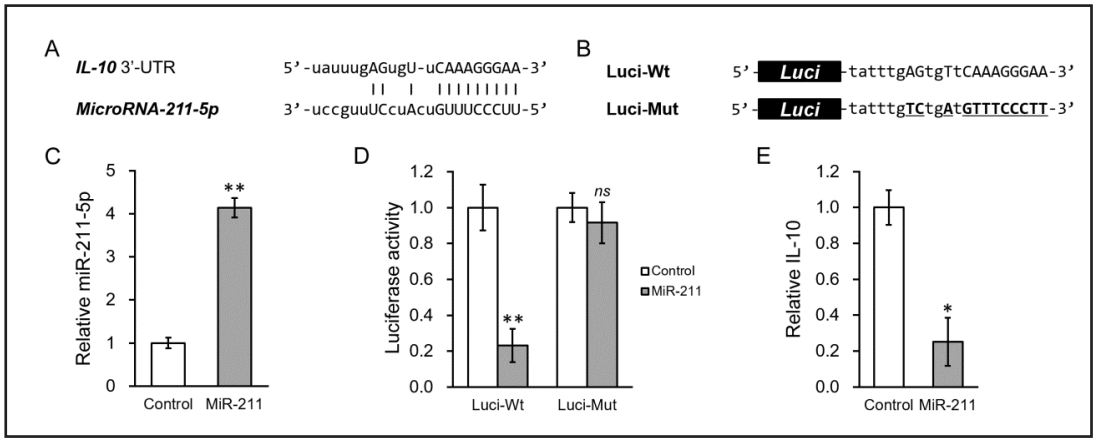


**Fig. 4.** MiR-211-5p directly targets 3'-UTR of IL-10 mRNA to inhibit its secretion from BALF-derived macrophages. (A) Predicted miR-211-5p targeting site (capitalized) on the 3'-UTR of IL-10 mRNA. (B) Wild type (Wt) and mutated version (Mut, mutated nucleotides were underlined) of miR-211-5p targeting sequence on IL-10 mRNA 3'-UTR were cloned to the downstream of a luciferase reporter gene (Luci), respectively. (C) Expressions of miR-211-5p were analyzed by mature miRNA assay in macrophages expressing either control miR or miR-211-5p mimic. (D) Luciferase activities of Luci-Wt and Luci-Mut constructs were assessed in macrophages expressing either control miR or miR-211-5p mimic. (E) IL-10 secretion from the macrophages expressing either control miR or miR-211-5p mimic, respectively, were analyzed by ELISA assay. Data were shown as mean±SD from at least three independent experiments. ** p<0.01, * p<0.05, ns p>0.05, compared to control.

*MiRNA expression profile in isolated BALF macrophages*

Our earlier data validated the ARDS rat model and characterized the corresponding inflammatory reactions in the lung tissues. Next, we sought to identify the candidate miRNA mechanistically involving in macrophage-mediated ARDS. For this purpose, we first interrogated the miRNA expression profiles in the macrophages isolated from both experimental groups of rats. In our comparative study, a number of miRNAs, including miR-211-5p, miR-137, miR-154, miR-204, miR-218, miR-317, miR-374, miR-488, miR-520, miR-1343 and miR-3073, showed consistent up-regulation (Fig. 3A). The preliminary results were further validated by the mature miRNA assays against the potential candidates. Although our

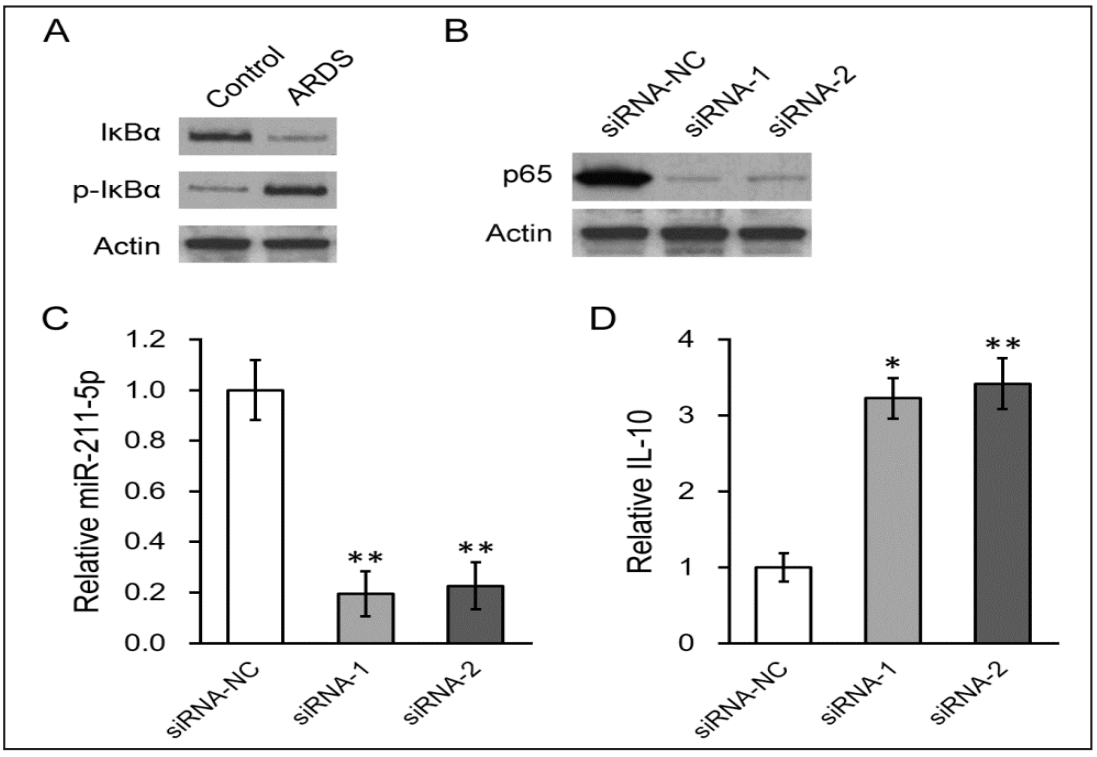


**Fig. 5.** NF-κB was activated in macrophages of ARDS rats, which was required for upregulating miR-211-5p expression and inhibiting IL-10 secretion. (A) Protein expressions of related proteins of NF-κB pathway in macrophages isolated from BALF of control and ARDS rats, respectively, were analyzed by Western blot. (B) Protein expressions of NF-κB subunit p65 were analyzed following its siRNA knockdown. (C) Expression of miR-211-5p was analyzed by mature miRNA assay following p65 siRNA knockdown. (D) IL-10 secretion was analyzed by ELISA assay following p65 siRNA knockdown. Data were shown as mean±SD from at least three independent experiments. ** $p<0.01$, * $p<0.05$, compared to control.

expression profiling data suggested several miRNAs were significantly up-regulated in our ARDS model, we decided to focus on miR-211-5p in view of its critical roles in inflammation [16-18]. Mature miRNA assay demonstrated a nearly 3-fold increase of miR-211-5p in ARDS rats in comparison with control group (Fig. 3B). Meanwhile, the secretory cytokines from BALF-isolated macrophages were interrogated with ELISA. As shown in Fig. 3C, IL-10 was dramatically inhibited in macrophages from ARDS rats compared to control rats, which prompted us to clarify whether miR-211-5p post-transcriptionally regulated IL-10.

*MiR-211-5p directly targets 3'-UTR of IL-10 mRNA to inhibit its secretion from BALF-derived macrophages*

We first set out to analyze the potential regulatory role of miR-211-5p on IL-10 expression using the miRanda algorithm [19]. As illustrated in Fig. 4A, we have identified putative targeting sequence of miR-211-5p in the 3'UTR region of IL-10. This regulatory effect was further experimentally confirmed by luciferase reporter assay. Either wild-type or the putative-sequence-mutated 3'UTR of IL-10 was cloned downstream into luciferase plasmid (Fig. 4B) and co-expressed with miR-211-5p. The exogenous introduction of miR-211-5p (Fig. 4C) markedly inhibited the luciferase activity with wild-type 3'UTR of IL-10 (Fig. 4D), this effect was further and directly confirmed by the reduction of secretory IL-10 in response to miR-211-5p expression in macrophages (Fig. 5E). However, mutation located in the putative target region severely impaired miR-211-5p mediated suppression on IL-10 expression and secretion (Fig. 4E). Our data provided evidence that IL-10 was a target gene of miR-211-5p in this setting.

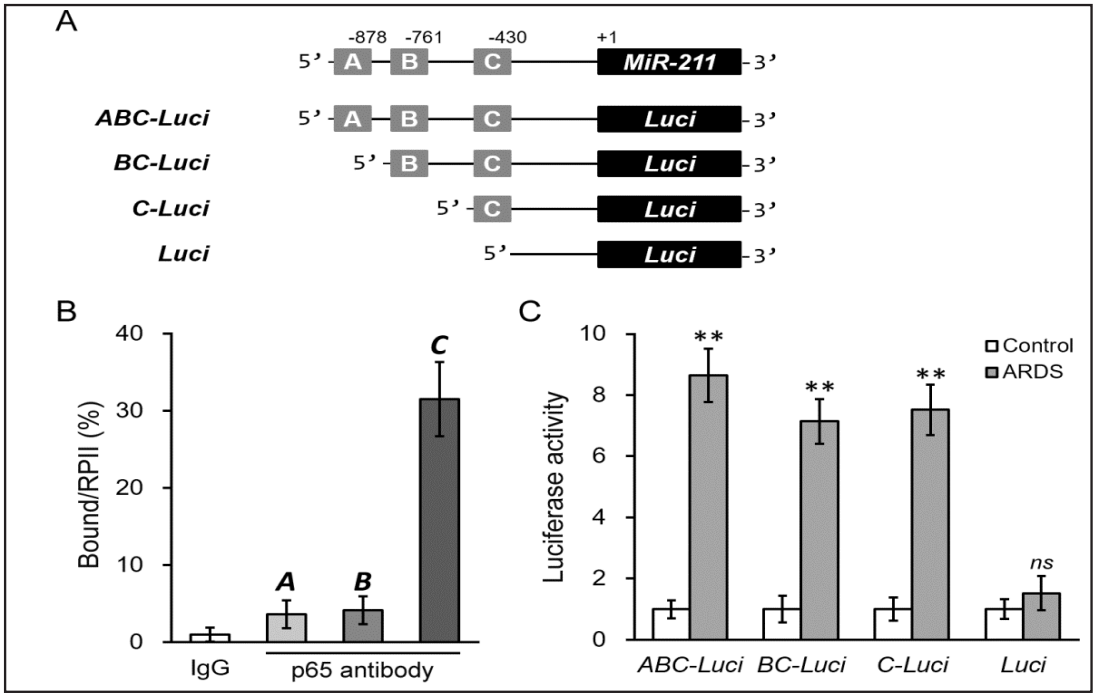


**Fig. 6.** NF-κB induced miR-211 expression by directly binding to its promoter region. (A) Promoter region of miR-211 contains three putative binding sites for p65, which were selectively cloned, as indicated, to the of upstream of a luciferase reporter open reading frame (Luci), (B) Binding of p65 to the each of the three sites on miR-211 promoter in macrophages was analyzed by ChIP assay, using control IgG and p65 antibody, respectively. (C) Luciferase activities of ABC-Luci, BC-Luci, C-Luci and Luci, as illustrated in panel (A), were analyzed in macrophages isolated from BALF of control and ARDS rats, respectively. Data were shown as mean±SD from at least three independent experiments. ** $p<0.01$, ns $p>0.05$, compared to control.

*NF-κB is activated in macrophages of ARDS rats and required for upregulating miR-211-5p expression and inhibiting IL-10 secretion*

Next, we sought to understand how miR-211-5p was regulated in BALF-derived macrophages. Since NF-κB is a crucial pathway in modulation of inflammatory reaction [20-22], here we first analyzed activation of NF-κB. Phosphorylated IκBα is the active form and was significantly induced in BALF-derived macrophages from ARDS rats, whereas the un-phosphorylated form was correspondingly decreased (Fig. 5A). Next, the effector of NF-κB pathway, p65, was specifically silenced by two independent siRNAs with satisfactory efficiency (Fig. 5B). Consequently, the endogenous expression of miR-211-5p was greatly suppressed by p65 knockdown (Fig. 5C). Moreover, the secreted IL-10 in the culture medium was markedly increased more than 3 times (Fig. 5D). Our data suggested that NF-κB signaling was aberrantly over-activated in BALF-derived macrophages from ARDS rats, which in turn stimulated miR-211-5p expression and consequently inhibited IL-10 expression and secretion.

*NF-κB induces miR-211 expression by directly binding to its promoter regions*

Our previous results demonstrated that siRNA mediated silencing of NF-κB significantly inhibited miR-211 expression. In view of its intrinsic property as a transcription factor, here we further investigated whether NF-κB directly bound to and transcriptionally stimulated miR-211 expression. Close inspection of miR-211 promoter region identified three putative NF-κB binding sites with the consensus sequence: GGRNNYYC (R-purine, Y-pyrimidine and N-any base) (Fig. 6A). We further demonstrated that NF-κB directly bound to motif C by ChIP assay with around 8-fold enrichment (Fig. 6B). The full-length miR-211 promoter-driven luciferase displayed around 9-times higher expression in BALF-derived macrophages from

ARDS than control rats. Consistent with our ChIP result, deletion in either A motif only or both A and B motifs in miR-211 promoter showed little impact on luciferase activity, respectively (Fig. 6C). Taken together, our data demonstrated the direct binding of NF-κB on the motif C within miR-211 promoter, which in turn activated its transcription.

## Discussion

The acute respiratory distress is a severe clinical complication potentially provoked by many diseases, which pathologically manifests as intensive inflammation [23]. However, the fundamental mechanism underlying the inflammatory response triggered and regulated during the course of disease is still elusive. Here we employed *in vivo* model to address this question. We first established the ARDS disease model in rats following the well-established protocol via intratracheal instillation of the cytotoxic LPS [14]. The dosed rat displayed apparent respiratory distress with declined gas exchange rate. Lung edema was induced upon LPS instillation as indicated by the wet/dry ratio of the lung tissues. We collected the BALF for further characterization and found significantly elevated protein contents, which was the distinct sign of pulmonary inflammation. Next, we have clarified the immune cell composition in the inflammatory situation. Total cells, macrophages, neutrophils and lymphocytes were remarkably enriched in the BALF from ARDS model rats, which consolidated the acute and intensive inflammatory response in LPS-stimulated animals. The macrophages are important mediator in both acute and chronic inflammation [15], here we selected this population of immune cells for further investigations. As miRNAs have been reported to serve as novel therapeutic targets in acute lung injury and ARDS [13], we adopted the strategy of miRNA microarray to interrogate the expression profile in ARDS-related inflammatory setting. The comparative study has identified multiple differentially expressed candidate miRNAs in ARDS vs control groups. The subsequent confirmatory phase validated the up-regulation of miR-211-5p in BALF-derived macrophages.

MiR-211 has been reported to play diverse roles in various physiological and pathological processes. For example, Mazar et al. demonstrated that miR-211 functioned as a metabolic switch in human melanoma cells [24]. In a case-control study, Sumbul et al. reported that miR-211 was up-regulated and associated with the poor prognosis in colorectal cancers [25]. MiR-211 has also been suggested as a tumor suppressor miRNA via inhibiting cell proliferation and invasion of gastric cancer by down-regulating SOX4 [26]. Intriguingly, IL-10Rα expression was demonstrated to be post-transcriptionally regulated by miR-211 along with the other two miRNAs in melanoma [16]. Most notably, several previous studies implicated the mechanistic involvement of miR-211 in inflammatory response. Li *et al.* proposed that miR-211/204 downregulation contributed to candidemia-induced kidney injury via derepressing Hmx1 expression [17]. Chen et al. identified a functional variant in the 3'UTR of angiopoietin-1 associated with the reduced risk of stroke due to partially impaired binding with miR-211 [18]. In agreement with these observations, our data demonstrated aberrantly up-regulated miR-211-5p in ARDS-related inflammation, which was also reversely correlated with declined secretion of IL-10 for the first time in LPS-induced animal model of ARDS to our best knowledge.

Like many well-defined miRNAs, the diverse target genes of miR-211 have been identified and characterized, including PP2Cm [18], Cyclin D1, CDK6 [27], SATB2 [28], CDC25B [29], NUAK1 [30], TGFβR II [31], CHD5 [32] and BRN2 [33]. Based on our preliminary finding, we employed the miRanda algorithm [19] to analyze the potential regulatory effect of miR-211-5p on IL-10. Combining algorithm prediction and experimental validation, we demonstrated that IL-10 was a novel target gene of miR-211-5p in ARDS-related macrophages, and over-expressed miR-211-5p suppressed expression and secretion of IL-10. Although we uncovered this regulatory mechanism in our ARDS pathological setting, it is possible that this miR-211-5p/IL-10 regulation may exist in other physiological conditions such as development.

IL-10 is the most important agent in the resolution of inflammation in airway via inhibiting the production of IFN-γ, IL-2 and nitric oxide [34]. Previous studies have indicated

the fundamental function of IL-10 in ARDS. For instance, Aisiku et al. reported that plasma IL-10, IL-6 and IL-8 were associated with development of ARDS in patients with severe traumatic brain injury [35]. Contradictorily, Parsons et al. reported that circulating IL-1ra and IL-10 levels were increased but not related to the development of ARDS in at-risk patients [36]. In contrast to the high level of peripheral IL-10, the secretory IL-10 from BALF-derived macrophages was significantly repressed due to up-regulation of miR-211-5p, therefore the resolution of the local inflammation was seriously delayed.

It's increasingly acknowledged that over-activated NF-κB pathway fundamentally underlies the pathogenesis of ARDS. For example, Li et al. characterized that he receptor for advanced glycation end products/NF-κB signaling mediated LPS-induced acute lung injury in neonate rat model [20], while angiotensin-converting enzyme 2 prevented LPS-induced rat lung injury via suppressing the ERK1/2 and NF-κB signaling pathways [21]. Song *et al.* demonstrated that recombinant human brain natriuretic peptide attenuated LPS-induced cellular injury in human fetal lung fibroblasts via inhibiting MAPK and NF-κB pathway activation [22]. In line with these observations, our study suggested that NF-κB pathway was aberrantly activated in BALF-derived macrophages in the ARDS rat model, which subsequently stimulated miR-211-5p expression and inhibited IL-10 expression and secretion, and consequently contributed to pathogenesis of ARDS. Our results highlighted the essential role of NF-κB /miR-211-5p/IL-10 signaling axis in ARDS-related inflammation, which might provide further understanding of the molecular mechanism underlying the disease.

## Disclosure Statement

The authors have nothing to disclose.

## References

1 Confalonieri M, Salton F, Fabiano F: Acute respiratory distress syndrome. Eur Respir Rev 2017;26: pii: 60116
2 Fanelli V, Ranieri VM: Mechanisms and clinical consequences of acute lung injury. Ann Am Thorac Soc 2015;12 Suppl 1:S3-8.
3 Villar J, Blanco J, Kacmarek RM: Current incidence and outcome of the acute respiratory distress syndrome. Curr Opin Crit Care 2016;22:1-6.
4 Crimi E, Slutsky AS: Inflammation and the acute respiratory distress syndrome. Best Pract Res Clin Anaesthesiol 2004;18:477-492.
5 Zhang Y, Guan L, Yu J, Zhao Z, Mao L, Li S, Zhao J: Pulmonary endothelial activation caused by extracellular histones contributes to neutrophil activation in acute respiratory distress syndrome. Respir Res 2016;17:155.
6 Bartel DP: MicroRNAs: genomics, biogenesis, mechanism, and function. Cell 2004;116:281-297.
7 Ambros V: The functions of animal microRNAs. Nature 2004;431:350-355.
8 Thum T, Galuppo P, Wolf C, Fiedler J, Kneitz S, van Laake LW, Doevendans PA, Mummery CL, Borlak J, Haverich A, Gross C, Engelhardt S, Ertl G, Bauersachs J: MicroRNAs in the human heart: a clue to fetal gene reprogramming in heart failure. Circulation 2007;116:258-267.
9 Insull W, Jr.: The pathology of atherosclerosis: plaque development and plaque responses to medical treatment. Am J Med 2009;122:S3-S14.
10 Romao JM, Jin W, Dodson MV, Hausman GJ, Moore SS, Guan LL: MicroRNA regulation in mammalian adipogenesis. Exp Biol Med (Maywood) 2011;236:997-1004.
11 Yonemori K, Kurahara H, Maemura K, Natsugoe S: MicroRNA in pancreatic cancer. J Hum Genet 2017;62:33-40.
12 Deshpande DA, Dileepan M, Walseth TF, Subramanian S, Kannan MS: MicroRNA Regulation of Airway Inflammation and Airway Smooth Muscle Function: Relevance to Asthma. Drug Dev Res 2015;76:286-295.
13 Cao Y, Lyu YI, Tang J, Li Y: MicroRNAs: Novel regulatory molecules in acute lung injury/acute respiratory distress syndrome. Biomed Rep 2016;4:523-527.

14 Hou S, Ding H, Lv Q, Yin X, Song J, Landen NX, Fan H: Therapeutic effect of intravenous infusion of perfluorocarbon emulsion on LPS-induced acute lung injury in rats. PLoS One 2014;9:e87826.
15 Arora S, Dev K, Agarwal B, Das P, Syed MA: Macrophages: Their role, activation and polarization in pulmonary diseases. Immunobiology 2017;10.1016/j.imbio.2017.11.001
16 Venza I, Visalli M, Beninati C, Benfatto S, Teti D, Venza M: IL-10Ralpha expression is post-transcriptionally regulated by miR-15a, miR-185, and miR-211 in melanoma. BMC Med Genomics 2015;8:81.
17 Li XY, Zhang K, Jiang ZY, Cai LH: MiR-204/miR-211 downregulation contributes to candidemia-induced kidney injuries via derepression of Hmx1 expression. Life Sci 2014;102:139-144.
18 Chen J, Yang T, Yu H, Sun K, Shi Y, Song W, Bai Y, Wang X, Lou K, Song Y, Zhang Y, Hui R: A functional variant in the 3'-UTR of angiopoietin-1 might reduce stroke risk by interfering with the binding efficiency of microRNA 211. Hum Mol Genet 2010;19:2524-2533.
19 Betel D, Koppal A, Agius P, Sander C, Leslie C: Comprehensive modeling of microRNA targets predicts functional non-conserved and non-canonical sites. Genome Biol 2010;11:R90.
20 Li Y, Wu R, Tian Y, Yu M, Tang Y, Cheng H, Tian Z: RAGE/NF-kappaB signaling mediates lipopolysaccharide induced acute lung injury in neonate rat model. Int J Clin Exp Med 2015;8:13371-13376.
21 Li Y, Zeng Z, Cao Y, Liu Y, Ping F, Liang M, Xue Y, Xi C, Zhou M, Jiang W: Angiotensin-converting enzyme 2 prevents lipopolysaccharide-induced rat acute lung injury via suppressing the ERK1/2 and NF-kappaB signaling pathways. Sci Rep 2016;6:27911.
22 Song Z, Zhao X, Liu M, Jin H, Cui Y, Hou M, Gao Y: Recombinant human brain natriuretic peptide attenuates LPS-induced cellular injury in human fetal lung fibroblasts via inhibiting MAPK and NF-kappaB pathway activation. Mol Med Rep 2016;14:1785-1790.
23 Shaver CM, Bastarache JA: Clinical and biological heterogeneity in acute respiratory distress syndrome: direct versus indirect lung injury. Clin Chest Med 2014;35:639-653.
24 Mazar J, Qi F, Lee B, Marchica J, Govindarajan S, Shelley J, Li JL, Ray A, Perera RJ: MicroRNA 211 Functions as a Metabolic Switch in Human Melanoma Cells. Mol Cell Biol 2016;36:1090-1108.
25 Sumbul AT, Gogebakan B, Bayram S, Batmaci CY, Oztuzcu S: MicroRNA 211 expression is upregulated and associated with poor prognosis in colorectal cancer: a case-control study. Tumour Biol 2015;36:9703-9709.
26 Wang CY, Hua L, Sun J, Yao KH, Chen JT, Zhang JJ, Hu JH: MiR-211 inhibits cell proliferation and invasion of gastric cancer by down-regulating SOX4. Int J Clin Exp Pathol 2015;8:14013-14020.
27 Xia B, Yang S, Liu T, Lou G: miR-211 suppresses epithelial ovarian cancer proliferation and cell-cycle progression by targeting Cyclin D1 and CDK6. Mol Cancer 2015;14:57.
28 Jiang G, Cui Y, Yu X, Wu Z, Ding G, Cao L: miR-211 suppresses hepatocellular carcinoma by downregulating SATB2. Oncotarget 2015;6:9457-9466.
29 Song GQ, Zhao Y: MicroRNA-211, a direct negative regulator of CDC25B expression, inhibits triple-negative breast cancer cells' growth and migration. Tumour Biol 2015;36:5001-5009.
30 Bell RE, Khaled M, Netanely D, Schubert S, Golan T, Buxbaum A, Janas MM, Postolsky B, Goldberg MS, Shamir R, Levy C: Transcription factor/microRNA axis blocks melanoma invasion program by miR-211 targeting NUAK1. J Invest Dermatol 2014;134:441-451.
31 Chu TH, Yang CC, Liu CJ, Lui MT, Lin SC, Chang KW: miR-211 promotes the progression of head and neck carcinomas by targeting TGFbetaRII. Cancer Lett 2013;337:115-124.
32 Cai C, Ashktorab H, Pang X, Zhao Y, Sha W, Liu Y, Gu X: MicroRNA-211 expression promotes colorectal cancer cell growth *in vitro* and *in vivo* by targeting tumor suppressor CHD5. PLoS One 2012;7:e29750.
33 Boyle GM, Woods SL, Bonazzi VF, Stark MS, Hacker E, Aoude LG, Dutton-Regester K, Cook AL, Sturm RA, Hayward NK: Melanoma cell invasiveness is regulated by miR-211 suppression of the BRN2 transcription factor. Pigment Cell Melanoma Res 2011;24:525-537.
34 Mosser DM, Zhang X: Interleukin-10: new perspectives on an old cytokine. Immunol Rev 2008;226:205-218.
35 Aisiku IP, Yamal JM, Doshi P, Benoit JS, Gopinath S, Goodman JC, Robertson CS: Plasma cytokines IL-6, IL-8, and IL-10 are associated with the development of acute respiratory distress syndrome in patients with severe traumatic brain injury. Crit Care 2016;20:288.
36 Parsons PE, Moss M, Vannice JL, Moore EE, Moore FA, Repine JE: Circulating IL-1ra and IL-10 levels are increased but do not predict the development of acute respiratory distress syndrome in at-risk patients. Am J Respir Crit Care Med 1997;155:1469-1473.